

**Evidence for the excited triplet of  $\text{Co}^{3+}$  in  $\text{LaCoO}_3$** 

S. Noguchi,\* S. Kawamata, and K. Okuda

*Graduate School of Engineering, Osaka Prefecture University, Sakai 599-8531, Japan*H. Nojiri<sup>†</sup> and M. Motokawa*Institute for Materials Research, Tohoku University, Sendai 980-8577, Japan*

(Received 5 April 2001; revised manuscript received 29 November 2001; published 5 September 2002)

The state excited from the ground singlet of  $\text{Co}^{3+}$  in  $\text{LaCoO}_3$  was investigated by submillimeter-wave electron spin resonance (ESR) measurements. Clear ESR signals with zero-field splitting were observed above 20 K for the first time. The activation energy is estimated to be  $\Delta \approx 140$  K, from the temperature dependence of the signal intensity and the resonance-width. The frequency and angular dependence of the signals were successfully analyzed by an effective spin-Hamiltonian with uniaxial anisotropy. The parameters obtained are  $g_{\parallel} = 3.35$ ,  $g_{\perp} = 3.55$ , and  $D = +4.90 \text{ cm}^{-1}$  for the effective spin  $S = 1$ . The results reveal that the first excited state is a triplet with a zero-field splitting of  $\text{Co}^{3+}$  in  $\text{LaCoO}_3$ .

DOI: 10.1103/PhysRevB.66.094404

PACS number(s): 76.30.Fc

**I. INTRODUCTION**

$\text{LaCoO}_3$  has attracted much attention in recent decades because of its anomalous successive changes of spin-states and unique magnetic behavior due to a highly covalent electronic state.<sup>1-20</sup> The ground state of  $\text{LaCoO}_3$ , at 4.2 K, is a nonmagnetic insulator due to the low-spin (LS) state of  $t_{2g}^6$  configuration with spin  $S = 0$ .<sup>1</sup> The first change of spin state is observed at around 100 K, where the susceptibility shows a broad peak, which implies a paramagnetic state above 100 K. The second change of spin state is evidenced by a plateau in the susceptibility at around 500 K, above which the Curie constant becomes large, showing the appearance of another magnetic spin state.<sup>2,3</sup> This anomalous change in spin state is associated with a semiconductor-metal transition.<sup>4-7</sup> The spin state above 500 K is now commonly recognized as a high-spin (HS) state of  $t_{2g}^4 e_g^2$  configuration with  $S = 2$ , shown by various experimental studies such as resistivity,<sup>4</sup> photoemission,<sup>5</sup> thermal expansion,<sup>6</sup> and specific heat.<sup>7</sup> The cause of the anomaly around 100 K, on the other hand, remains an issue and has been the subject of a debate. In the following, we call the state between 100 K and 500 K, the “intermediate spin” (IS) state.

Theoretical models for the IS state have been proposed, such as an IS state of  $t_{2g}^5 e_g^1$  configuration with  $S = 1$ ,<sup>8,9</sup> a LS+HS ordered state on an enlarged double cell,<sup>10</sup> and others.<sup>11</sup> Recently, Radwanski and Ropka have pointed out that the trigonal crystal-field (CF) and the spin-orbit (SO) coupling are important in forming the nonmagnetic ground state caused by the splitting of the HS state.<sup>12</sup> In this model, the lowest level of the fictitious spin  $S' = 1$  is split into a nonmagnetic singlet ground state and a magnetic excited doublet state with a gap of 125 K.

A potentially useful experimental approach to understanding the IS state is to investigate the excited states of  $\text{LaCoO}_3$ . Electron spin resonance (ESR) measurement is a powerful tool for observing a spin-state of a ground state or a state excited from a ground singlet. However, there have to date been no ESR measurements on the  $\text{Co}^{3+}$  ion since the spin-

relaxation rate of the paramagnetic  $\text{Co}^{3+}$  ion is generally too fast to allow the signal to be observed. However, submillimeter-wave ESR measurements under a pulsed magnetic field have the advantages of wide field-sweep and high-frequency measuring, which makes it possible to observe a broad signal due to a short relaxation time. In the present work, we have made submillimeter-wave ESR measurements of  $\text{Co}^{3+}$  in a  $\text{LaCoO}_3$  single crystal at temperatures below 70 K in order to identify the energy levels excited from the ground singlet. We believe these are the first measurements of the ESR signals of  $\text{Co}^{3+}$ .<sup>13</sup>

**II. EXPERIMENT**

High-quality single crystals of  $\text{LaCoO}_3$  were grown by a floating zone method from a sintered polycrystalline rod in an infrared imaging furnace. They were confirmed to be a single phase of a rhombohedrally distorted structure by x-ray powder diffraction. The hexagonal lattice parameters of  $a = 5.428 \text{ \AA}$  and  $c = 13.065 \text{ \AA}$  were in accord with previously published data.<sup>6,14,15</sup> A sample of a single crystal domain was cut into a half-disk shape of 2 mm diam and 1 mm thickness and used in the ESR measurements.

The submillimeter-wave ESR measurements were performed using a pulsed magnet up to 30 T in a temperature range from 4.2 to 70 K.<sup>21</sup> Radiation in the range from 135 to 1400 GHz was supplied by an optically pumped far-infrared laser and backward-traveling-wave tube. Measurements were done by a simple transmission method with a Faraday configuration where the propagation vector of the incident radiation is aligned parallel to the external field. The sample was mounted in the light pipe at the center of magnet, together with a DPPH ( $\alpha$ -diphenyl- $\beta$ -picryl-hydrazyl) whose signals were simultaneously monitored as a standard.

**III. RESULTS**

The ESR absorption spectra of  $\text{LaCoO}_3$  for various frequencies were obtained at several temperatures between 4.2 and 70 K for the field direction along the [001], “cubic,” and

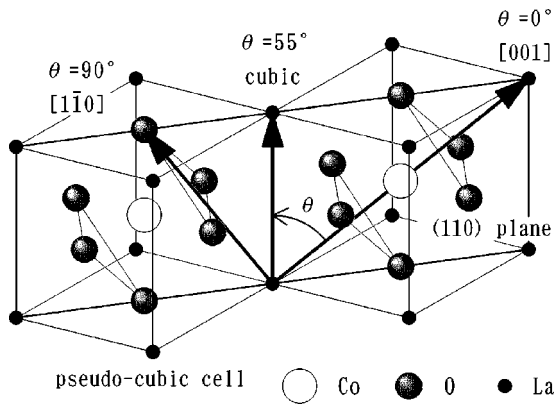


FIG. 1. Crystal structure, local coordinates around Co<sup>3+</sup>, and notation of the angle  $\theta$  between the field direction and [001] axis in the (110) plane of LaCoO<sub>3</sub>.

[ $\bar{1}10$ ] axes, where “cubic” corresponds to the pseudo-cubic axis as illustrated in Fig. 1. Typical examples obtained at 525 GHz for [001] and at 429 GHz for the “cubic” axis are shown in Figs. 2(a) and 2(b), respectively. For the [001] direction, two large absorptions appear at 8.2 and 14.4 T above 20 K, denoted by  $f_1$  and  $f_2$ , respectively. With increasing temperature, they grow in intensity and resonance-width, and subsequently become a broad single absorption at 70 K. Sharp signals at 16.3 and 18.4 T observed at 4.2 K decrease in intensity abruptly with increasing temperature, suggesting paramagnetic impurities such as Co<sup>2+</sup> due to oxygen deficiency or crystal imperfection. For this reason, we do not consider the signals at low temperatures. A sharp signal at 18.8 T comes from the DPPH marker. For the “cubic” direction, a large absorption denoted by  $f_1, f_2$  and a small absorption denoted by  $f_0$  are observed above 20 K at 8.7 and 4.0 T, respectively.

The temperature dependence of the integrated intensity  $I$

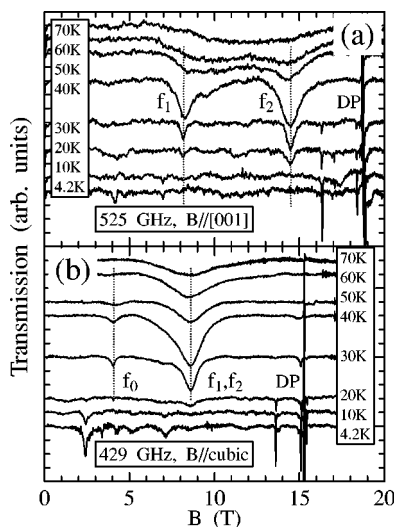


FIG. 2. ESR spectra of LaCoO<sub>3</sub> at various temperatures between 4.2 and 70 K (a) with a frequency of 525 GHz for  $B$  parallel to [001], and (b) with a frequency of 429 GHz for  $B$  parallel to the “cubic” axis. The sharp signals labeled DP are from DPPH.

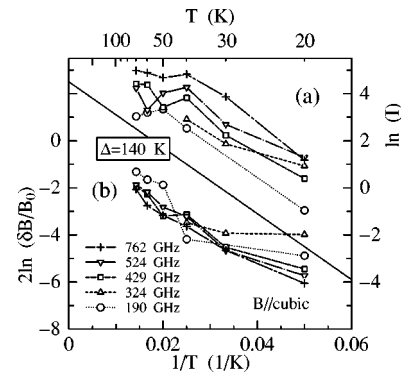


FIG. 3. Temperature dependence of (a) the absorption intensity and (b) the resonance-width as logarithmically plotted against  $1/T$  at several frequencies for  $B$  parallel to the “cubic” axis. The solid line corresponds to the activation energy  $\Delta = 140$  K.

of the absorption was examined to check that it follows the activation formula  $I = I_0 \exp(-\Delta/T)$ , where  $\Delta$  is the energy gap between the excited and the ground states. The logarithmic plot of  $I$  to  $1/T$  is shown in Fig. 3(a). The data follow the activation formula below 40 K at all frequencies. Above 50 K, the intensity shows a saturated tendency, which suggests that the spin-lattice relaxation time becomes long due to large energy absorption. Since it is known that  $\delta B$  is proportional to the square root of the spin concentration due to the dipolar broadening,<sup>22</sup> the resonance-width  $\delta B$  was also checked against the activation formula  $(\delta B/B_0)^2 \propto \exp(-\Delta/T)$ , where  $B_0$  is the resonance field. The data follow the activation formula above 30 K at all frequencies as shown in Fig. 3(b). The energy gap is estimated to be  $\Delta \approx 140$  K from both plots.

In order to estimate the  $g$ -value of LaCoO<sub>3</sub>, the frequency dependence of the resonance-fields was plotted as a frequency-field diagram for  $B$  parallel to [001], [ $\bar{1}10$ ] and the “cubic” axis. As shown in Fig. 2, the resonance-fields are almost independent of temperature in the range between 30 and 50 K. A frequency-field diagram for  $B$  parallel to [001] at 50 K is shown in Fig. 4. With increasing frequency, the resonance-fields of  $f_1$  and  $f_2$  linearly increase, separated by 6 T, which suggests that the signals come from the triplet state with a zero-field splitting (ZFS). The linear dependence of the resonance-field suggests that the [001] axis is the principal axis of the trigonal CF originating in the ZFS. The

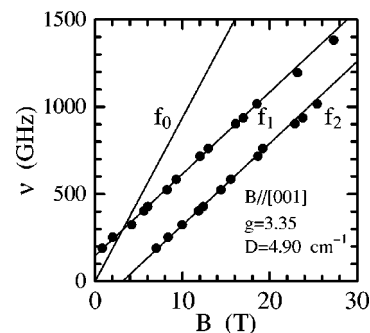


FIG. 4. Frequency-field diagram for [001] of LaCoO<sub>3</sub> at 50 K. The solid lines represent calculated curves.

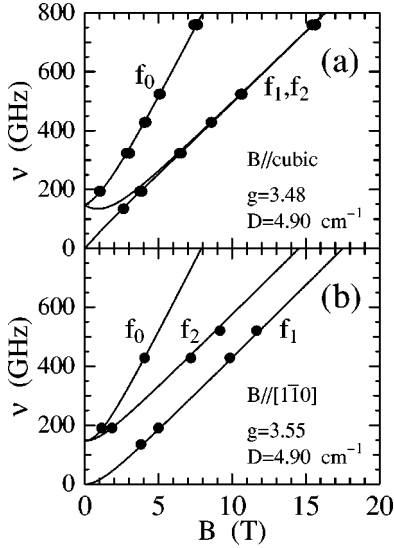


FIG. 5. Frequency-field diagram of  $\text{LaCoO}_3$  (a) for the “cubic” axis in the temperature range 30–50 K and (b) for  $[1\bar{1}0]$  at 30 K. The solid lines represent calculated curves.

$g$ -value along the  $[001]$  axis and the ZFS energy  $D$  are roughly estimated to be  $g_{\parallel}=3.4$  and  $D=4.9 \text{ cm}^{-1}$ , from the slope and the intercept of the resonance-field line. In previous data reported by our group, six ESR signals were observed due to the multidomain sample.<sup>13</sup> It is easy to form multidomains in  $\text{LaCoO}_3$  because there are four equivalent directions allowing distortion from a cubic to a rhombohedral structure. In this study, however, only two signals were observed, which suggests the sample used in the measurements has a single domain. Frequency-field diagrams for  $B$  parallel to the “cubic” axis and  $B$  parallel to  $[1\bar{1}0]$  were also obtained and are shown in Figs. 5(a) and 5(b), respectively.

ESR spectra for 429 GHz at 30 K were measured for several field directions in the  $(110)$  plane of  $\text{LaCoO}_3$ , as shown in Fig. 6, where  $\theta$  is defined as the angle from the  $[001]$  axis.  $f_1$  and  $f_2$  were assigned by the relative signal intensity. Another small signal  $f_0$  appears in low field regions and shows little angular dependence. The angular dependence of the resonance fields of  $f_0$ ,  $f_1$ , and  $f_2$  is summarized

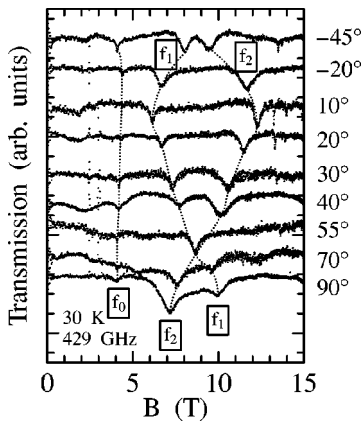


FIG. 6. ESR spectra of  $\text{LaCoO}_3$  with a frequency of 429 GHz at 30 K for various field directions from the  $[001]$  axis.

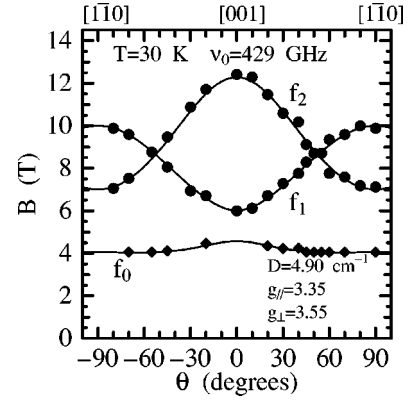


FIG. 7. Angular dependence of the resonance fields for 429 GHz at 30 K. The solid lines represent calculated curves.

in Fig. 7. The resonance fields of  $f_1$  and  $f_2$  show an approximately  $\sin 2\theta$  dependence with a crossing at  $55^\circ$ . The  $f_0$  signal, which comes from the transition with the selection rule  $\Delta M=2$ , can be observed as a weakly allowed transition, whose intensity is smaller by a factor of  $(D/g\mu_B H_0)^2$ .<sup>23</sup>

Before discussing the relation between the ESR results and the spin-state of  $\text{Co}^{3+}$ , we present a tentative analysis of the data summarized in Figs. 4, 5, 7 by a simple effective spin-Hamiltonian with a uniaxial CF splitting,

$$\mathcal{H} = \mu_B S \tilde{g} H_0 + D \{S_z^2 - S(S+1)/3\}, \quad (3.1)$$

where  $S$  and  $S_z$  are spin matrices of the effective spin  $S=1$ . The  $z$  direction is defined as the  $[001]$  trigonal axis.  $H_0$  is an applied magnetic field, and  $\mu_B$  is the Bohr magneton.  $\tilde{g}$  is a  $g$ -tensor assumed to be uniaxial anisotropic whose principal values are given by  $(g_{\parallel}, g_{\perp}, g_{\perp})$ , where  $g_{\perp}, g_{\parallel}$ , and  $D$  are the fitting parameters. This is quite a natural formula and explains the results sufficiently.

The energy eigenvalue of the Hamiltonian,  $W$  is easily calculated and obtained by solving the following equation:

$$w^3 - (\frac{1}{3} + h_{\parallel}^2 + h_{\perp}^2)w + \frac{2}{27} - \frac{1}{3}(2h_{\parallel}^2 - h_{\perp}^2) = 0, \quad (3.2)$$

where

$$w = W/D, \quad (3.3)$$

$$h_{\parallel} = g_{\parallel} \mu_B H_0 \cos \theta / D, \quad (3.4)$$

$$h_{\perp} = g_{\perp} \mu_B H_0 \sin \theta / D. \quad (3.5)$$

From these calculations, a best fit was obtained with the values for the parameters  $g_{\parallel} = 3.35 \pm 0.05$ ,  $g_{\perp} = 3.55 \pm 0.05$ , and  $D = 4.90 \pm 0.02 \text{ cm}^{-1}$ , as drawn by the solid curves in Figs. 4, 5, 7, although the sign of  $D$  is indefinite in the calculations.

The sign of  $D$  is determined from the relative intensities of the  $f_1$  and  $f_2$  signals. The schematic relations between the energy levels and the ESR spectra for the principal axis are shown in Fig. 8. If  $D > 0$  then the signal intensity for a high resonance-field is larger than that for a low field because the

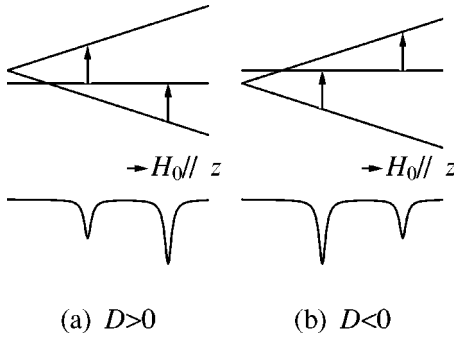


FIG. 8. Schematic relation between energy level and ESR spectra for principal axis in the case of (a)  $D > 0$  and (b)  $D < 0$ .

spins populate the low energy levels to a greater degree. As shown in Fig. 2, the intensity of  $f_2$  is always larger than that of  $f_1$  for  $B$  parallel to  $[001]$ . Therefore, the sign of  $D$  is determined to be *positive* in this case. This is consistent with the spectra for the other directions as shown in Fig. 6.

#### IV. DISCUSSIONS

The results are summarized by an energy level scheme for  $\text{LaCoO}_3$  shown in Fig. 9 for  $B$  parallel to  $[001]$ . We discuss the results in detail in the following.

##### A. Ground state

As shown in Fig. 2, the main signals due to the excited state are observed without overlapping of the impurity signals. This is an advantage over other statistical measurements such as susceptibility. Thus, the ground singlet is confirmed by the fact that the signals  $f_0$ ,  $f_1$ , and  $f_2$  are never observed at 4.2 K. Recently, Radwanski and Ropka have proposed that the singlet is caused by the trigonal CF and the SO coupling in the frame of the HS state as mentioned above.<sup>12</sup> In this case, only one ESR signal without ZFS should be observed as a transition in the magnetic doublet, which is incompatible with the experimental facts. Therefore, the ground singlet originates from the LS state, as discussed by several researchers.<sup>1,3-10,13,16-20</sup>

##### B. Excited triplet

In the preliminary ESR measurements up to 120 K, a broad absorption at 70 K gradually broadens and eventually

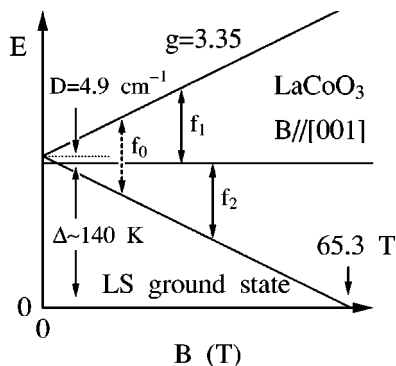


FIG. 9. Energy level scheme of  $\text{LaCoO}_3$  for  $B$  parallel to  $[001]$ .

vanishes with increasing temperature while no drastic change is observed in the temperature range. This broadening suggests that the spin relaxation time becomes short with increasing temperature through the spin-lattice interaction due to a phonon and possibly an electron hopping in the present compounds. That there is no drastic change suggests that the magnetic anomaly at 100 K is a rather gradual change. Therefore, the excited triplet is significant to explain the nature of the anomaly at 100 K and the IS state.

At first, we note that the  $g$ -value obtained is almost coincident with that of  $\text{Fe}^{2+}$  in  $\text{MgO}$ , which is well known through ESR studies to be a typical example of a  $d^6$  electron system with a HS state in an octahedral CF.<sup>24</sup> In that case, the 15-fold degenerate orbital triplet is separated into three levels with the fictitious spins  $S' = 1, 2$ , and 3 by the SO interaction and the state of  $S' = 1$  is the lowest. The  $g$ -value is deduced, mainly from the effective Landé factor and the orbital-reduction due to covalency, to be  $g = 3 + \frac{1}{2}\kappa$ , where  $\kappa = 0.8-0.9$  is the orbital-reduction parameter.<sup>24,25</sup> Thus, the  $g$ -value of the excited triplet of  $\text{Co}^{3+}$  in  $\text{LaCoO}_3$  does not conflict with the state of  $S' = 1$  of the HS point-charge model, although the covalency due to a  $d-\sigma$  hybridization is significant in the compound. The small anisotropy in the  $g$ -value is consistent with the experimental results of magnetic torque and susceptibility measurements on a  $\text{LaCoO}_3$  single crystal done by our group.<sup>26</sup>

Next we discuss the  $D$  value, which is mainly connected to the trigonal CF. Ito *et al.* used a trigonal CF parameter  $\delta$ , which is the same as  $D$ , of value  $\delta = -120 \text{ cm}^{-1}$  to reproduce the characteristic features of susceptibility and NMR measurements.<sup>16</sup> The value  $D = +4.90 \text{ cm}^{-1}$  obtained from the ESR measurements is much smaller than  $\delta$  and has the opposite sign. The small value implies that the trigonal CF is strongly reduced by the orbital reduction effect of the covalency due to  $d-\sigma$  hybridization as a factor of  $\kappa^2$ . The positive sign is natural in this case under the trigonal CF in the point charge model.

A numerical comparison with  $D$  values for other perovskite oxides may be useful. For example, it has been reported that  $D = 0.0490$  and  $-0.0555 \text{ cm}^{-1}$  for  $\text{Fe}^{3+}$  and  $\text{Cr}^{3+}$  in  $\text{LaAlO}_3$ , respectively, which crystallize in a rhombohedrally distorted perovskite structure.<sup>27</sup> The  $D$  value in  $\text{LaCoO}_3$  is much larger than those in  $\text{LaAlO}_3$ . Some factors such as the characteristic of the excited state, a possible IS( $t_{2g}^5 e_g^1$ ) state,<sup>8,9,19</sup> and heavily mixed  $d^6$  and  $d^7L$  states<sup>17</sup> may cause this difference.

By using the energy level scheme, the temperature dependence of the susceptibility was calculated. The position of the peak at 90 K was well reproduced although the absolute value is about three times larger than the experimental data. This conflict has been previously pointed out in the analysis of NMR and susceptibility measurements.<sup>16</sup> Thus, the temperature dependence of the susceptibility is not sufficiently explained by the energy level scheme. This remains one of the problems in understanding the IS state.

##### C. Activation energy

The activation energy estimated from analyzing the temperature dependence of the susceptibility is distributed over

the range 150–310 K.<sup>4,16–18</sup> Recently, Kobayashi *et al.* have reported an energy gap of 180 K from the temperature dependence of the nuclear-spin relaxation measurements below  $T \sim 35$  K.<sup>20</sup> Our result is roughly consistent with these data. As shown in Fig. 9, the lowest level of the excited triplet crosses over the ground singlet at 65.3 T, which is almost in accordance with the metamagnetic transition field of 67 T reported by Katori *et al.*<sup>28</sup> Therefore, a good estimation is  $\Delta \approx 140$  K.

## V. CONCLUDING REMARKS

An energy level scheme of the ground singlet and the excited triplet was experimentally determined from the ESR measurements of  $\text{Co}^{3+}$  in  $\text{LaCoO}_3$ . The characteristic parameters of the excited triplet were found to be  $g_{\parallel} = 3.35$ ,  $g_{\perp} = 3.55$ , and  $D = +4.90 \text{ cm}^{-1}$  for the effective

spin  $S = 1$ . The activation energy was estimated to be  $\Delta \approx 140$  K. The  $g$ -value does not conflict with the state of  $S' = 1$  of the HS point-charge model. The results of this study should contribute to the building of a realistic microscopic model of the IS state.

## ACKNOWLEDGMENTS

This work was partly supported by a Grant-in-Aid for Scientific Research on Priority Areas “Novel Quantum Phenomena in Transition Metal Oxides – Spin·Charge·Orbital Coupled Systems –” (No. 12046253) from the Ministry of Education, Science, Sports, and Culture of Japan. A part of this work was carried out under the Visiting Researcher’s Program of the Institute for Material Research at Tohoku University.

\*Electronic address: noguchi@pe.osakafu-u.ac.jp

<sup>†</sup>Present address: Department of Physics, Okayama University, Okayama, 700-8530, Japan.

<sup>1</sup>K. Asai, P. Gehring, H. Chou, and G. Shirane, *Phys. Rev. B* **40**, 10982 (1989); K. Asai, O. Yokokura, N. Nishimori, H. Chou, J.M. Tranquada, G. Shirane, S. Higuchi, Y. Okajima, and K. Kohn, *ibid.* **50**, 3025 (1994).

<sup>2</sup>R.R. Heikes, R.C. Miller, and R. Mazelsky, *Physica (Amsterdam)* **30**, 1600 (1964).

<sup>3</sup>G.H. Jonker, *J. Appl. Phys.* **37**, 1424 (1966).

<sup>4</sup>S. Yamaguchi, Y. Okimoto, H. Taniguchi, and Y. Tokura, *Phys. Rev. B* **53**, R2926 (1996); Y. Tokura, Y. Okimoto, S. Yamaguchi, H. Taniguchi, T. Kimura, and H. Takagi, *ibid.* **58**, R1699 (1998).

<sup>5</sup>M. Abbate, J.C. Fuggle, A. Fujimori, L.H. Tjeng, C.T. Chen, R. Potze, G.A. Sawatzky, H. Eisaki, and S. Uchida, *Phys. Rev. B* **47**, 16124 (1993).

<sup>6</sup>K. Asai, A. Yoneda, O. Yokokura, J.M. Tranquada, G. Shirane, and K. Kohn, *J. Phys. Soc. Jpn.* **67**, 290 (1998).

<sup>7</sup>S. Stølen, F. Grønvdal, H. Brinks, T. Atake, and H. Mori, *Phys. Rev. B* **55**, 14103 (1997).

<sup>8</sup>R.H. Potze, G.A. Sawatzky, and M. Abbate, *Phys. Rev. B* **51**, 11501 (1995).

<sup>9</sup>M.A. Korotin, S.Yu. Ezhov, I.V. Solovyev, V.I. Anisimov, D.I. Khomskii, and G.A. Sawatzky, *Phys. Rev. B* **54**, 5309 (1996).

<sup>10</sup>M. Zhuang, W. Zhang, and N. Ming, *Phys. Rev. B* **57**, 10705 (1998).

<sup>11</sup>S. Ramasesha, T.V. Ramakrishnan, and C.N.R. Rao, *J. Phys. C* **12**, 1307 (1979).

<sup>12</sup>R.J. Radwański and Z. Ropka, *Solid State Commun.* **112**, 621 (1999); *Physica B* **281&282**, 507 (2000).

<sup>13</sup>K. Okuda, S. Kawamata, K. Nakahigashi, H. Ishibashi, M. Ha-

yashi, H. Ohta, H. Nojiri, and M. Motokawa, *J. Magn. Magn. Mater.* **177-181**, 1375 (1998).

<sup>14</sup>P.M. Raccach and J.B. Goodenough, *Phys. Rev.* **155**, 932 (1967).

<sup>15</sup>G. Thornton, B.C. Tofield, and A.W. Hewat, *J. Solid State Chem.* **61**, 301 (1986).

<sup>16</sup>M. Itoh, M. Sugahara, I. Natori, and K. Motoya, *J. Phys. Soc. Jpn.* **64**, 3967 (1995); M. Itoh, M. Mori, M. Sugahara, T. Yamauchi, and Y. Ueda, *Physica B* **230-232**, 756 (1997).

<sup>17</sup>T. Saitoh, T. Mizokawa, A. Fujimori, M. Abbate, Y. Takeda, and M. Takano, *Phys. Rev. B* **55**, 4257 (1997).

<sup>18</sup>S. Yamaguchi, Y. Okimoto, and Y. Tokura, *Phys. Rev. B* **55**, R8666 (1997).

<sup>19</sup>N.Y. Vasanthacharya and P. Ganguly, *Bull. Mater. Sci.* **5**, 307 (1983).

<sup>20</sup>Y. Kobayashi, N. Fujiwara, S. Murata, K. Asai, and H. Yasuoka, *Phys. Rev. B* **62**, 410 (2000).

<sup>21</sup>H. Nojiri, H. Kageyama, K. Onizuka, Y. Ueda, T. Asano, Y. Ajiro, and M. Motokawa, *J. Phys. Soc. Jpn. Suppl. B* **69**, 83 (2000).

<sup>22</sup>C. Kittel and E. Abrahams, *Phys. Rev.* **90**, 238 (1953).

<sup>23</sup>A. Abragam and B. Bleaney, *Electron Paramagnetic Resonance of Transition Ions* (Clarendon, Oxford, 1970), p. 21.

<sup>24</sup>W. Low and M. Weger, *Phys. Rev.* **118**, 1119 (1960); **118**, 1130 (1960).

<sup>25</sup>A. Abragam and B. Bleaney, *Electron Paramagnetic Resonance of Transition Ions* (Clarendon, Oxford, 1970), p. 443.

<sup>26</sup>S. Noguchi, S. Kawamata, and K. Okuda (unpublished).

<sup>27</sup>D.R. Taylor, J. Owen, and B.M. Wanklyn, *J. Phys. C* **6**, 2592 (1973).

<sup>28</sup>H. Aruga Katori, T. Goto, H. Kawano, and H. Yoshizawa, Meeting Abstracts of the Physical Society of Japan, 1994, Vol. 49, p. 4.